Available online at www.sciencedirect.com
ScienceDirect
Trans. Nonferrous Met. Soc. China 23(2013) 2923−2928
Transactions of Nonferrous Metals Society of China
www.tnmsc.cn

Cyclic oxidation and hot corrosion of Al_2O_3 or Y_2O_3-dispersed low-temperature chromizing coating

Hai-jun ZHANG, Jian-feng SUN, Yue-bo ZHOU

College of Materials Science and Engineering, Heilongjiang Institute of Science and Technology, Harbin 150027, China

Received 10 September 2012; accepted 8 January 2013

Abstract: Chromium coatings with and without Al_2O_3 or Y_2O_3 particles were prepared by chromizing the as-deposited Ni-film with and without Al_2O_3 or Y_2O_3 particles using a conventional pack-cementation method at 800 °C. The cyclic oxidation at 800 °C and hot corrosion in molten 75% Na_2SO_4+25% NaCl at 800 °C of the three different chromizing coatings were investigated. The effects of Al_2O_3 or Y_2O_3 on the cyclic oxidation and hot corrosion behavior of the chromizing coatings were discussed. Microstructure results show that the codeposited Al_2O_3 or Y_2O_3 particles significantly retard the grain growth of the chromizing coating, which increases the cyclic oxidation and hot corrosion resistance of the chromizing coatings, due to the more rapid formation of purer and denser chromia scale.

Key words: electrodeposition; chromizing coating; cyclic oxidation; hot corrosion

1 Introduction

Chromizing is one of the widely used surface coating technologies to economically improve high temperature oxidation, corrosion resistance of components [1−6]. Various chromizing processes have been developed, such as pack-cementation method, molten-salt technique, and vacuum chromizing process. Pack-cementation has been one of the easiest and cheapest processes to obtain the chromizing coatings since the early 1950s. Unfortunately, the pack-cementation was normally performed at temperatures above 1000 °C, and limited by the diffusion and reaction kinetics involved, which has a detrimental effect on the mechanical properties of workpieces. Therefore, reducing pack-cementation temperature is required for widespread application of the chromizing coatings. Recently, a novel ultrafine-grained chromizing coating with improved oxidation resistance [7] due to "reactive element effect (REE)" [8], produced using pack cementation method at low temperature, on the electrodeposited Ni−CeO_2 nanocomposite coatings was developed. Oxidation of alloys or coatings with addition of RE or RE oxide has been widely reported [9−12]. Various theories to elucidate the REE have been put forward but still are in dispute [9]. ZHOU et al [13,14] also found that the chromizing process was mainly controlled by inward chromium diffusion at low temperatures. The co-deposited Al_2O_3 or Y_2O_3 particles significantly retarded the grain growth of the chromizing coatings, which enhanced Cr diffusion to the oxidation front and consequently accelerated the formation of a continuous pure chromia scale in a short transient stage of oxidation. In this work, cyclic oxidation at 800 °C and hot corrosion in molten 75% Na_2SO_4+25% NaCl at 800 °C of the three different chromizing coatings were studied in order to reveal the effect of Al_2O_3 or Y_2O_3 on the formation of thermally formed oxide scales in various environments.

2 Experimental

2.1 Preparation of coating

Samples with dimensions of 15 mm×10 mm×2 mm were cut from an electrolytic nickel plate. They were ground with a final 800# SiC paper. After ultrasonic cleaning in acetone, they were first electrodeposited with Ni, Ni−Al_2O_3 or Ni−Y_2O_3 composite from a nickel sulfate bath containing certain content of Al_2O_3 or Y_2O_3 particles. Chromizing on the samples coated with the Ni−Al_2O_3, Ni−Y_2O_3 and Ni film was carried out using

Foundation item: Project (11531319) supported by Scientific Research Fund of Heilongjiang Provincial Education Department, China
Corresponding author: Hai-jun ZHANG; Tel: +86-451-88036526; E-mail: zhanghaijun0418@163.com
DOI: 10.1016/S1003-6326(13)62815-0

pack cementation at 800 °C for 5 h in a pure Ar atmosphere [13,14]. Surface morphologies shown in Fig. 1 and transmission electron microscopy (TEM) results [13,14] exhibit that the codeposited Y_2O_3 or Al_2O_3 particles retard the grain growth of the chromizing coating, which enhances the diffusion of chromium during pack cementation and leads to higher Cr content in the Al_2O_3 or Y_2O_3-dispersed chromium coating than the Al_2O_3 or Y_2O_3-free chromizing coating at a given distance from the coating surface [13,14].

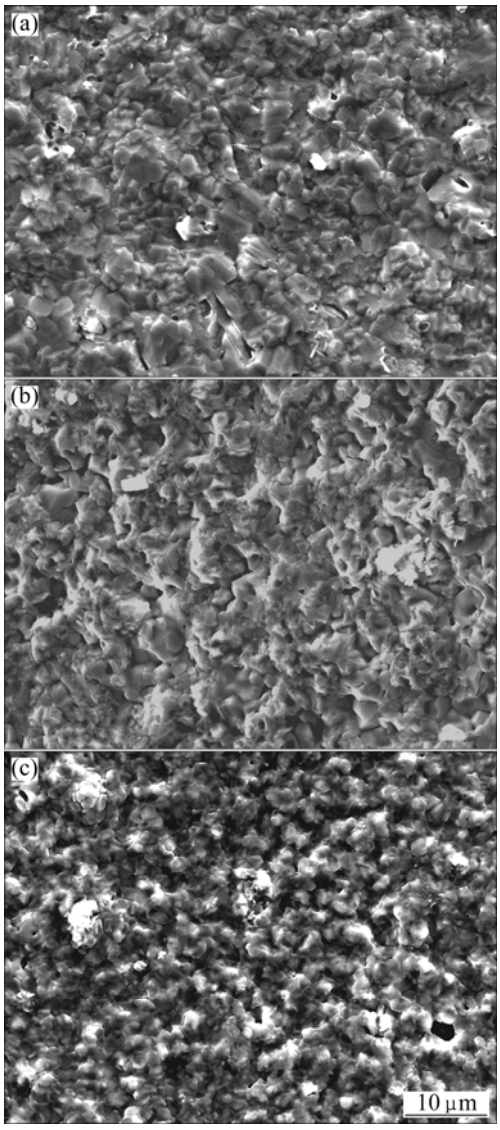

Fig. 1 SEM images showing surface morphologies of various chromizing coatings on Ni film (a), Ni−Y_2O_3 (b) and Ni−Al_2O_3 (c) composite coatings

2.2 Experimental method

Cyclic oxidation at 900 °C up to 100 h in air was performed by automatically lifting samples from the hot zone of a vertical furnace after 1 h exposure period followed with 10 min cooling to room temperature. During the exposure, the specimens were taken out after fixed time intervals, cooled in air, and weighed.

The hot corrosion test was carried out in 75% Na_2SO_4 + 25% NaCl in a muffle furnace in an ambient atmosphere at 800 °C, which is over the liquidus temperature of ~620 °C for the mixed salt. Before exposure, specimens were preheated, followed by deposition with 1.6 mg/cm^2 salt film using hand-brushed techniques as provided elsewhere [7,8]. Then the specimens were placed in a crucible for hot corrosion test. The specimens were taken out, cleaned, weighed and recoated with salt after several hours, and the whole time for the hot corrosion test was 30 h.

The mass changes of the specimens were measured using an electrobalance with a detection limit of 0.01 mg. After oxidation/corrosion, the phase, surface and cross-sectional morphologies of scale formed were examined using scanning electron microscopy (SEM) with energy dispersive X-ray analysis (EDAX) and X-ray diffraction (XRD).

3 Results

3.1 Cyclic oxidation

The mass change vs time curves of cyclic oxidation of the three chromizing coatings during 100 h cyclic oxidation in air at 800 °C are shown in Fig. 2. No scale spallation occurred for three samples during the entire thermal cycling. The results demonstrate that the oxidation rate of Y_2O_3 or Al_2O_3-dispersed chromium coatings is profoundly slower than that of the chromizing coating on the Ni film.

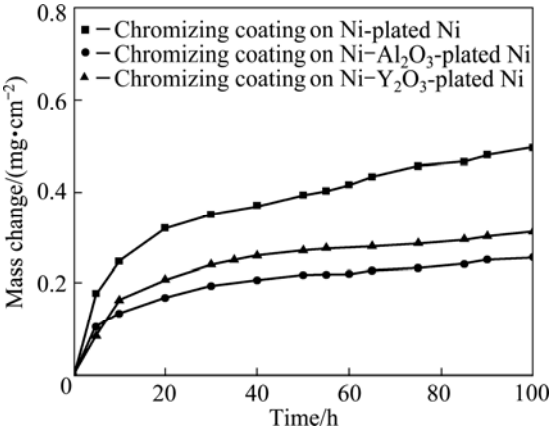

Fig. 2 Cyclic oxidation curves of various chromizing coatings after oxidation at 800 °C for 100 h

The XRD analysis indicates that the oxide scales on the three coatings are single phase Cr_2O_3. However, for oxidation of the Y_2O_3 or Al_2O_3-dispersed chromium coating a peak from the coating substrate noticeably appears, indicating that the chromia scale formed is thinner in this case, which is also visually confirmed by SEM/EDAX.

Figure 3 shows the SEM top-views of the chromia scales formed on various coatings after 100 h cyclic oxidation. Compared with the chromia feature on the chromized Ni (Fig. 3(a)), the chromia grains on the Y_2O_3 or Al_2O_3-dispersed chromium coating have a noticeably finer-grain structure (Figs. 3(b) and (c)), especially the latter.

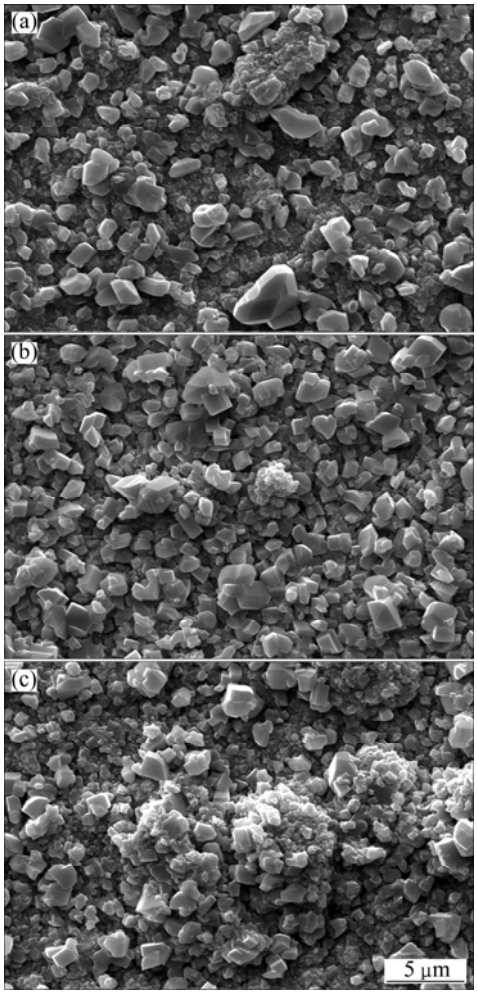

Fig. 3 SEM images showing surface morphologies of various chromizing coatings on Ni film (a), Ni−Y_2O_3 (b) and Ni−Al_2O_3 (c) composite coatings after cyclic oxidation at 800 °C for 100 h

By comparing the cross-sectional morphologies of the chromia scale on the different coatings after cyclic oxidation in Fig. 4, it can be seen that the oxide scale thickness formed is reduced due to the addition of Al_2O_3 or Y_2O_3 particles, which is consistent with the oxidation kinetics in Fig. 2.

3.2 Hot corrosion

Figure 5 shows the mass change vs time curves for the three chromizing coatings at 800 °C under the molten Na_2SO_4−NaCl mixture. The mass change is the net result of the combination of mass gain by oxide scale formation during exposure and mass loss due to scale exfoliation during cooling (the mass loss as a result of salt evaporation was not considered because its value

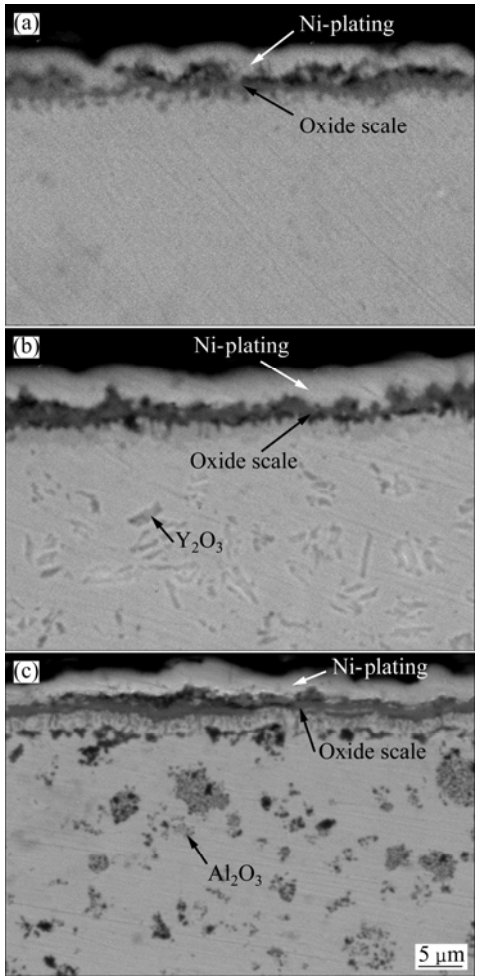

Fig. 4 SEM images showing cross-sectional morphologies of various chromizing coatings on Ni film (a), Ni−Y_2O_3 (b) and Ni−Al_2O_3 (c) composite coatings after cyclic oxidation at 800 °C for 100 h

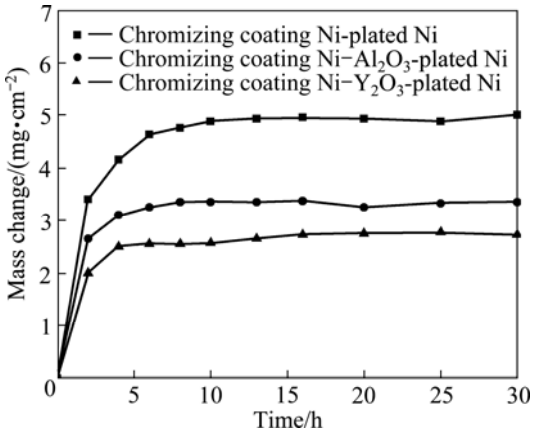

Fig. 5 Mass change vs time curves of various chromizing coatings in molten 75% Na_2SO_4 + 25% NaCl at 800 °C for 30 h

was almost the same for all samples). Clearly, the Y_2O_3 or Al_2O_3-dispersed chromium coatings exhibited an apparently low scaling rate during a short transient stage of oxidation.

Figure 6 shows the XRD patterns of the samples after 30 h hot corrosion. The scales on the three chromizing coatings have single phase. However, for oxidation of the Y_2O_3 or Al_2O_3-dispersed chromizing coating a preferential growth in the [110] direction and a peak from the coating substrate noticeably appear, suggesting that the chromia scale formed is thinner, which is also visually confirmed by SEM.

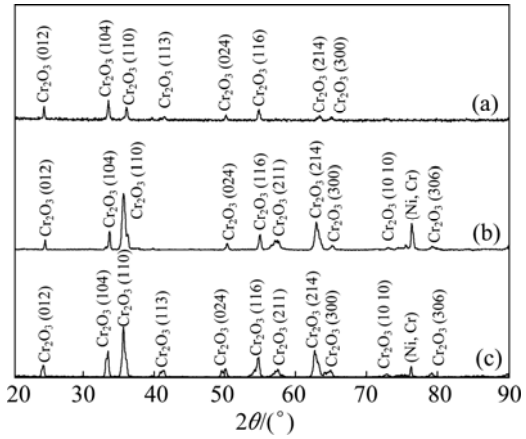

Fig. 6 XRD patterns of various chromizing coatings on Ni film (a), Ni−Y_2O_3 (b) and Ni−Al_2O_3 (c) composite coatings after hot corrosion at 800 °C

Figure 7 shows the SEM top-views of the scales formed on the three chromizing coatings after hot corrosion at 800 °C for 30 h in the molten Na_2SO_4−NaCl mixture. Clearly, fine equiaxed-grain oxides shown in Fig. 7(a) formed on the surface of the scale formed on the chromium coating on Ni film. While, with the addition of Y_2O_3 particles, some flake-like oxides particles occurred, as shown in Fig. 7(b). However, large flake-like oxide particles formed on the Al_2O_3-dispersed chromium coatings, as shown in Fig. 7(c). The formation of flake-like oxides may be the result of the preferred growth of the oxide on the {110} orient planes as mentioned above.

Figure 8 presents the cross-sectional morphologies of various samples after hot corrosion. Clearly, a thicker porous chromia scale with significant internal corrosion forms on the Y_2O_3 or Al_2O_3-free chromizing coating. The internal corrosion products are sulfides. In contrast, the chromia scale formed on the Y_2O_3 or Al_2O_3-dispersed chromizing coating is very thin and significant internal corrosion does not occur, which agree well with the XRD results in Fig. 6. From Figs. 8(b) and (c), it can be also found that a more significant growth of flake-like chromia scale on the Al_2O_3-dispersed chromium

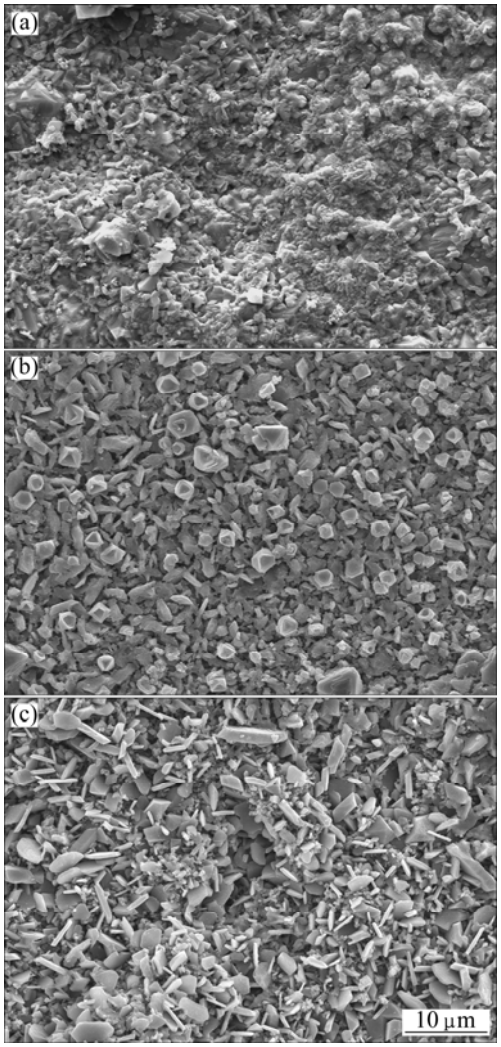

Fig. 7 SEM images showing surface morphologies of various chromizing coatings on Ni film (a), Ni−Y_2O_3 (b) and Ni−Al_2O_3 (c) composite coatings after hot corrosion at 800 °C

coatings is visible, which is consistent with the surface morphologies in Fig. 7(c).

4 Discussion

In this work, all chromized coatings on various samples are chromia former. However, cyclic oxidation and hot corrosion tests show that the scaling rate of the Y_2O_3 or Al_2O_3-dispersed chromizing coating is slower than that of the chromizing coating developed on Ni film, particularly in the first 5−10 h. The difference of scaling rate at the early stage demonstrates that the codeposited Y_2O_3 or Al_2O_3 particles have an important influence on the growth of chromia. Surface morphologies shown in Fig. 1 and transmission electron microscopy (TEM) results [13,14] exhibit that the codeposited Y_2O_3 or Al_2O_3 particles retard the grain growth of the chromizing coating. The increased grain boundaries are available sites for chromia nucleation

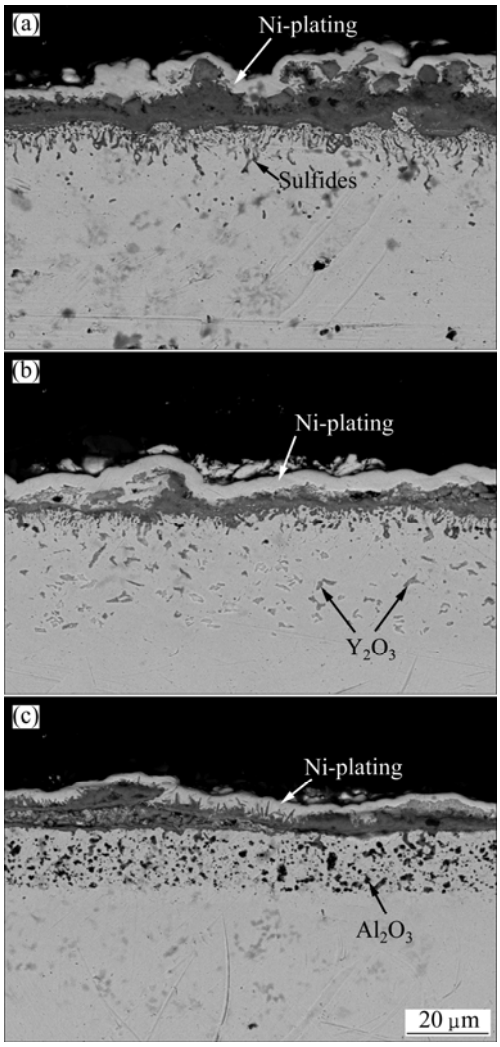

Fig. 8 SEM images showing cross-sectional morphologies of various chromizing coatings on Ni film (a), Ni−Y_2O_3 (b) and Ni−Al_2O_3 (c) composite coatings after hot corrosion at 800 °C

at onset of oxidation. The increased chromia nuclei formed on grain boundaries and dispersed Y_2O_3 or Al_2O_3 particles on the coating surface shorten the time for their linkage through the oxide lateral growth. After the establishment of the continuous chromia scale, the scale growth rate should be faster on the Y_2O_3 or Al_2O_3-dispersed chromizing coating because the chromia scale is finer, especially on the Y_2O_3-dispersed chromizing coating. The case, however, is not seen from the scaling kinetics, suggesting that grain-boundary diffusion of Cr cations is hindered to a great extent. The reason may be that the chromia scale is incorporated by Y ions released from the dispersed Y_2O_3 particles when they are incorporated into the growing scale [15]. Once being incorporated into the growing scale, they would potentially improve the oxidation resistance through blocking the dominant grain boundary outward diffusion of chromium [15], leading to a decrease of oxidation and more rapid formation of a purer and denser chromia scale at a short transient oxidation stage. ZHANG et al [7] reported that the more rapid formation of a continuous chromia scale leads to better protection of the metal against attack by aggressive species in molten salts. Although all chromizing coatings are chromia former in this work, the Y_2O_3 or Al_2O_3-free chromizing took a long time to form a continuous chromia layer, during which the molten salt attacked the coatings through the following route [16−20]: the molten salt first penetrated the growing oxide scale through defects such as pores and microcracks and arrived at the scale/alloy interface; SO_4^{2-} was then reduced by the following chemical equilibrium:

$$2SO_4^{2-} = 2O^{2-}+3O_2+2S$$

The inward penetration of sulfur caused the formation of the internal sulfides, as seen from Fig. 8(a). In contrast, significant internal sulfides did not appear in the Y_2O_3 or Al_2O_3-dispersed chromizing coating due to the more rapid formation of a continuous chromia scale with fine grain structure. The oxide layer with fine grain size can then easily release the thermal stress, therefore preventing crack propagation. Besides, the Y_2O_3 particles could play a role in retarding the outward diffusion of Ni [20]. Thus, the effect of synergistic dissolution could be minimised. In addition, the inward diffusion of sulphur could be retarded by the trapping effect [21] contributed by Y_2O_3 particles in the chromizing coating.

5 Conclusions

1) The codeposited Y_2O_3 or Al_2O_3 particles significantly retard the grain growth of the chromizing coatings by anchoring the movement of grain boundaries;

2) The refinement of the grain significantly improves the cyclic oxidation and hot corrosion resistance of the chromizing coatings through enhancing Cr diffusion to the oxidation front and consequently accelerating the formation of a continuous pure chromia scale at a short transient stage of oxidation.

References

[1] LEE J W, DUH J G, TSAI S Y. Corrosion resistance and microstructural evaluation of the chromized coating process in a dual phase Fe−Mn−Al−Cr alloy [J]. Surface and Coatings Technology, 2002, 153: 59−66.

[2] WANG Z B, LU J, LU K. Wear and corrosion properties of a low carbon steel processed by means of SMAT followed by lower temperature chromizing treatment [J]. Surface and Coatings Technology, 2006, 201: 2796−2801.

[3] ZHU L, PENG X, YAN J, WANG F. Oxidation of a novel chromium coating with CeO_2 dispersions [J]. Oxid Met, 2004, 62: 411−426.

[4] YAN J, PENG X, WANG F. Oxidation of a novel CeO_2-dispersion strengthened chromium coating in simulated coal-combustion gases

[J]. Mater Sci Eng A, 2006, 426: 266−273.
[5] PENG X, YAN J, DONG Z, XU C, WANG F. Discontinuous oxidation and erosion-oxidation of a CeO_2-dispersion-strengthened chromium coating [J]. Corrosion Science, 2010, 52: 1863−1873.
[6] PENG X, YAN J, ZHENG L, WANG F. Oxidation of a novel CeO_2-dispersed chromium coating in wet air [J]. Materials and Corrosion, 2011, 62: 514−520.
[7] ZHANG H, PENG X, ZHAO J, WANG F. Prior electrodeposition of nanocrystalline Ni−CeO_2 film fabricating an oxidation-resistant chromized coating on carbon steels [J]. Electrochemical and Solid-State Letters C, 2007, 10(3): 12−15.
[8] PFEIL B. Improvement in heat-resisting alloys: UK 459848[P]. 1937.
[9] MOON D P. Role of reactive elements in alloy protection [J]. Mater Sci Tech, 1989, 5: 754−763.
[10] CUEFF R, BUSCAIL H, CAUDRON E, ISSARTEL C, RIFFARD F. Oxidation behaviour of Kanthal A1 and Kanthal AF at 1173 K: Effect of yttrium alloying addition [J]. Applied Surface Science, 2003, 207: 246−254.
[11] LI M S, HOU P Y. Improved Cr_2O_3 adhesion by Ce ion implantation in the presence of interfacial sulfur segregation [J]. Acta Materialia, 2007, 55: 443−453.
[12] MITRA S K, ROY S K, BOSE S K. Improvement of nonisothermal oxidation behavior of Fe and Fe−Cr alloys by superficially applied reactive oxide coatings [J]. Oxid Met, 1990, 34: 101−121.
[13] ZHOU Y B, CHEN H, ZHANG H, WANG Y. Preparation and Oxidation of an Y_2O_3-dispersed chromizing coating by pack-cementation at 800 °C [J]. Vacuum, 2008, 82: 748−753.
[14] ZHOU Y B, CHEN H Y, ZHANG H J, WANG Y D. Oxidation of an Al_2O_3-dispersion chromizing coating by pack-cementation at 800 °C [J]. Transactions of Nonferrous Metals Society of China, 2008, 18: 598−602.
[15] PINT B A. Experimental observations in support of the dynamic segregation theory to explain the reactive-element effect [J]. Oxid Met, 1996, 45: 1−37.
[16] GOEBEL J A, PETTIT F S. Na_2SO_4-induced accelerated oxidation of nickel [J]. Met Trans, 1970, 1: 1943−1954.
[17] GOEBEL J A, PETTIT F S, GOWARD G W. Mechanisms for the hot corrosion of nickel-based alloy [J]. Met Trans, 1973, 4: 261−278.
[18] LI M H, SUN X F, HU W Y, GUAN H R, CHEN S G. Hot corrosion of a single crystal-Ni-based superalloy by Na-salts at 900 °C [J]. Oxid Met, 2006, 65 (1−2): 137−150.
[19] ZHANG C, PENG X, ZHAO, WANG F. Hot Corrosion of an electrodeposited Ni−11% Cr nanocomposite under molten Na_2SO_4−K_2SO_4−NaCl [J]. Journal of the Electrochemical Society B, 2005, 152(9): 321−326.
[20] RAPP R A. Hot corrosion of materials: A fluxing mechanism [J]. Corrosion Science, 2002, 44: 209−221.
[21] LEES D G. On the reasons for the effects of dispersions of stable oxides and additions of reactive elements on the adhesion and growth-mechanisms of chromia and alumina scales-the “sulfur effect” [J]. Oxid Met, 1987, 27: 75−81.

Al_2O_3 和 Y_2O_3 改性的低温渗铬涂层的循环氧化和热腐蚀性能

张海军，孙俭峰，周月波

黑龙江科技学院 材料科学与工程学院，哈尔滨 150027

摘 要: 采用在 Ni 基上复合电镀 Ni−Al_2O_3 和 Ni−Y_2O_3 复合涂层后在 800 °C 下扩散渗铬的方法，分别制备了 Al_2O_3 和 Y_2O_3 改性渗铬涂层。采用相同的工艺在单 Ni 镀层上直接渗铬，获得一种不含氧化物粒子的渗铬涂层。分析了 Al_2O_3 和 Y_2O_3 影响渗铬涂层的氧化和腐蚀性能的机理。组织结构分析表明，Al_2O_3 和 Y_2O_3 能明显抑制在渗铬过程中涂层晶粒的长大。800 °C 循环和 75% Na_2SO_4+25% NaCl 混合盐腐蚀试验结果表明：与在单 Ni 镀层上直接渗铬相比，Al_2O_3 和 Y_2O_3 改性的渗铬涂层所具有的细晶结构促进了保护性氧化物形成元素 Cr 沿晶界向氧化前沿的快速扩散，从而有利于致密保护性 Cr_2O_3 氧化膜的快速形成，使得改性的渗铬涂层表现出更优异的抗循环氧化和混合盐热腐蚀性能。

关键词: 电镀；渗铬涂层；循环氧化；热腐蚀

(Edited by Xiang-qun LI)